Study of the ^{56}Ni$(d,p)^{57}$Ni Reaction and the Astrophysical ^{56}Ni$(p,\gamma)^{57}$Cu Reaction Rate

K. E. Rehm,[1] F. Borasi,[1] C. L. Jiang,[1] D. Ackermann,[1] I. Ahmad,[1] B. A. Brown,[2] F. Brumwell,[1] C. N. Davids,[1] P. Decrock,[1] S. M. Fischer,[1] J. Görres,[3] J. Greene,[1] G. Hackmann,[1] B. Harss,[1] D. Henderson,[1] W. Henning,[1] R. V. F. Janssens,[1] G. McMichael,[1] V. Nanal,[1] D. Nisius,[1] J. Nolen,[1] R. C. Pardo,[1] M. Paul,[4] P. Reiter,[1] J. P. Schiffer,[1] D. Seweryniak,[1] R. E. Segel,[5] M. Wiescher,[3] and A. H. Wuosmaa[1]

[1]*Argonne National Laboratory, Argonne, Illinois 60439*
[2]*Michigan State University, East Lansing, Michigan 48824*
[3]*University of Notre Dame, South Bend, Indiana 46556*
[4]*Hebrew University, Jerusalem, Israel*
[5]*Northwestern University, Evanston, Illinois 60208*

(Received 29 August 1997)

The single-particle character of states outside the doubly magic (radioactive) nucleus ^{56}Ni has been determined through a measurement of the (d,p) neutron transfer reaction using inverse kinematics. From the spectroscopic factors of the low-lying states in ^{57}Ni, the astrophysically interesting yield for the ^{56}Ni(p,γ) reaction to the mirror nucleus ^{57}Cu has been calculated, utilizing charge symmetry. The rate for this reaction in the temperature range typical of novae, supernovae, and x-ray bursts is found to be more than 10 times higher than previously assumed. [S0031-9007(97)05085-0]

PACS numbers: 25.60.Je, 21.10.Pc, 26.30.+k, 27.40.+z

In the nuclear shell model, the magic number 28 is the first that requires the introduction of a strong spin-orbit interaction. Indeed, as was recognized in the formulation of the shell model, in the absence of spin-orbit coupling, the magic numbers 2, 8, and 20 would still occur, but 28 would be absent. The special character of the $N = Z = 28$ ^{56}Ni nucleus also accounts for the fact that ^{56}Fe is the most abundant heavy element in the Universe. Yet, ^{56}Ni is the first doubly magic $N = Z$ nucleus that is not stable ($T_{1/2} = 6.1$ d). Over the years, this feature has hampered studies of the properties of nuclear levels relevant to the $N = Z = 28$ shell gaps. For example, only very recently has the transition probability to the first excited state of ^{56}Ni been measured, using a ^{56}Ni radioactive beam [1]. Unlike other doubly magic nuclei such as ^{40}Ca with $N = Z = 20$, the $N = Z = 28$ shell gap does not result in a particularly small $B(E2)$ value for the lowest 2^+ state.

The shell-model description of nuclei near shell gaps benefits much from single-nucleon transfer reactions which provide a sensitive way to assert the single-particle character of low-lying states. The first three states in ^{57}Ni at $E_x = 0$, 0.768, and 1.113 MeV are known to have spin parities of $3/2^-$, $5/2^-$, and $1/2^-$. They are followed by another group of negative parity states $(5/2^-, 7/2^-, 3/2^-, \ldots)$ starting at 2.4 MeV. The problem is whether the lowest three states are predominantly single particle in character or whether this strength is fragmented (as it is, e.g., for the $3/2^-$ state in ^{41}Ca [2]). Admixtures to the low-lying states have been suggested on the basis of gamma decay properties of the excited states in ^{57}Ni [3]. These transition rates, however, are sensitive to even small admixtures in the wave functions and no definitive conclusion about the magnitudes of the admixtures can be drawn from the γ-ray data.

Reactions with ^{56}Ni are also of considerable interest in astrophysics. The isotope ^{56}Ni is produced via helium burning in the core of massive stars, in supernova explosions, and in explosive hydrogen burning [rapid proton (rp) process] [4], where, in a series of radiative proton capture reactions followed by β^+ decays, nuclei up to ^{56}Ni and beyond are produced. The small Q value ($Q = 0.695$ MeV) for the proton capture reaction on ^{56}Ni makes this nucleus a "waiting point" for the reaction flow towards heavier nuclei. For a realistic determination of the astrophysical reaction rate, detailed information on the structure of nuclei around $A = 56$ is required. In this paper, we discuss the measurement of the inverse $d(^{56}\mathrm{Ni}, p)^{57}$Ni reaction using a radioactive ^{56}Ni beam to determine the spectroscopic factors of low-lying states in ^{57}Ni. It is the first such measurement on a doubly magic nucleus outside the valley of stability.

The measurement was carried out at the ATLAS accelerator at Argonne National Laboratory. The ^{56}Ni material was produced via the ^{58}Ni$(p, p2n)^{56}$Ni reaction with a 50 MeV proton beam from the injector of the Intense Pulsed Neutron Source, also at Argonne. A small ^{58}Ni pellet (3 mm diameter, 2 mm thick, 99.6% enriched) was bombarded for 24 h with a 16 μA proton beam. Taking into account the cross section for the $(p, p2n)$ reaction [5] and the 12 mm diameter of the beam spot, a fraction of about 5×10^{-6} of the ^{58}Ni nuclei was converted into ^{56}Ni. The sample, already mounted in a Cu insert for the SNICS negative ion sputter source [6], was installed in the ion source of the tandem injector at ATLAS. The use of a negative-ion source and the selection of mass 56 strongly reduces the contribution of the stable isobar ^{56}Fe in the ion beam because of the low yield of Fe^- ions. The other isobar, ^{56}Co($T_{1/2} = 78.8$ d), which is produced in the sample

 0031-9007/98/80(4)/676(4)$15.00

through the ^{58}Ni$(p, 2pn)$ reaction, is difficult to remove in the accelerator, since the mass difference $\Delta M/M$ between ^{56}Ni and ^{56}Co is only 3.5×10^{-5}. Chemical separation could reduce the contribution of Fe and Co substantially, but this adds complexity and the separation cannot be complete, since ^{56}Co is the decay product of ^{56}Ni. The experiment was, therefore, carried out with a mixed beam of ^{56}Fe, ^{56}Co, and ^{56}Ni ions.

The beam that was extracted from the negative ion source and injected into the tandem accelerator contained 3×10^7 ^{56}Ni$^-$ ions/sec and about a factor of 7 more of the isobaric contaminant ^{56}Co. After stripping in the terminal of the tandem accelerator, the mass 56^{10+} beam was accelerated to an energy of 250 MeV with the superconducting linear accelerator section of ATLAS. The ^{56}Ni beam intensity on the target, averaged over a running time of 3.7 d, was 2.5×10^4/sec. While measurements with a stable ^{58}Ni beam gave a total transport efficiency (including stripping in the terminal of the tandem accelerator) of 4.9%, a transport efficiency of only 0.1% was achieved in this first experiment with ^{56}Ni. This was caused, in part, by the lack of a stable feedback signal needed to synchronize the bunching system of the accelerator.

The experiment was performed with a 500 μg/cm^2 CD_2 target located in the scattering chamber of the Fragment Mass Analyzer (FMA) [7]. The inset of Fig. 1 shows a schematic of the experimental setup. The protons emitted at backward angles from the $d(^{56}\text{Ni}, p)^{57}$Ni reaction were detected in a large Si detector array consisting of a position sensitive annular detector and six 5×5 cm^2 Si strip detectors (strip width 1 mm), covering a total solid angle of 2.8 sr. To separate the (d, p) reactions on ^{56}Ni from those induced by the ^{56}Co and ^{56}Fe beam impurities, the reaction products were identified by their mass and nuclear charge at the focal plane of the FMA in coincidence with protons. For the Z identification of the reaction products, it was necessary to use a passive absorber [8] consisting of a stack of ten Au foils with a total thickness of 7 mg/cm^2 (mounted 39 mm downstream from the target) that slowed down the Fe, Co, and Ni particles differently. The measurement of the energy E and the time of flight in the focal plane of the FMA, together with an energy loss ΔE signal from an ionization chamber, allowed us to identify the three isobaric components. A ΔE-E spectrum from the ionization chamber measured for incident mass 56 ions in their 23^+ charge state is shown in the bottom part of Fig. 1.

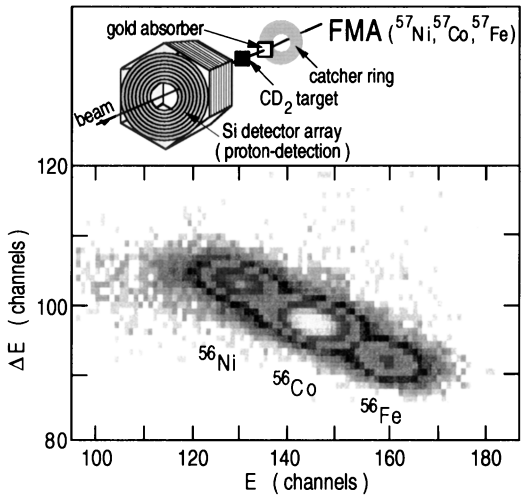

FIG. 1. (top) Schematic of the experimental setup used for measuring angular distributions for the $d(^{56}\text{Ni}, p)^{57}$Ni reaction in inverse kinematics. (bottom) ΔE-E_{res} spectrum measured with the ionization chamber in the focal plane of the FMA for a mixed beam of ^{56}Fe, ^{56}Co, and ^{56}Ni.

The integrated beam intensity was determined by collecting the ^{56}Ni and ^{56}Co particles elastically scattered from the Au absorber on a circular ring covering the angular range between $\theta = 4.5°-11.9°$ and by measuring the accumulated activity after the experiment with a calibrated Ge detector. Corrections were applied for the ^{56}Ni decay and for the time dependence of the exposure profile. The uncertainties of these corrections are estimated to $\pm 10\%$. The full experimental setup was tested by measuring the inverse reaction $d(^{28}\text{Si}, p)^{29}$Si with a 125 MeV ^{28}Si beam that was also used for tuning the ATLAS accelerator. Further details will be given in a forthcoming paper [9].

Figure 2(a) presents a Q-value spectrum for protons from the $d(^{56}\text{Ni}, p)$ reaction as measured with the annular Si detector that covers the angular range $\theta = 147°-162°$ in coincidence with ^{57}Ni ions detected in the FMA. In the center-of-mass system, this range corresponds to forward angles for a (d, p) reaction, where transitions to

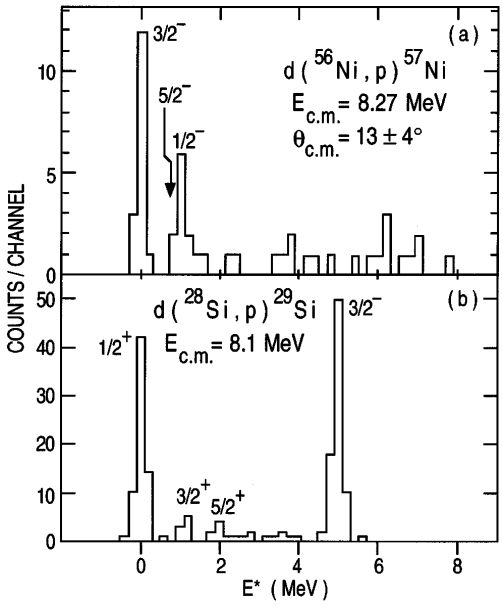

FIG. 2. (a) Q-value spectrum measured with the annular detector (see Fig. 1) for the $d(^{56}\text{Ni}, p)^{57}$Ni reaction at $E(^{56}\text{Ni}) = 250$ MeV. (b) Q-value spectrum for the $d(^{28}\text{Si}, p)^{29}$Si reaction. In this angle range, only $l = 0, 1$ states are strongly populated.

low-spin states ($l = 0, 1$) should be strongly populated. Indeed, the spectrum is dominated by the transitions to the $3/2^-$ ($E_x = 0$ MeV) and the $1/2^-$ ($E_x = 1.113$ MeV) states in ^{57}Ni. The yields for states at $E_x = 2.5$ and $E_x = 3.8$ MeV are considerably smaller, indicating little single-particle strength for low-spin states in ^{57}Ni at higher excitation energy. The spectrum is quite different from the one obtained for the $d(^{28}\mathrm{Si}, p)^{29}\mathrm{Si}$ calibration reaction, where a strong population of the high-lying $2p_{3/2}$ state at $E_x = 4.9$ MeV is observed [see Fig. 2(b)].

The angular distributions for the first three states in ^{57}Ni are presented in Fig. 3. The uncertainties in the measured differential cross sections include the statistical errors as well as uncertainties associated with beam current determination and detection efficiency. The charge-state distribution for Fe, Co, and Ni ions in the focal plane of the FMA was measured with mass 56 isobars. The transport efficiency through the FMA was calculated with the programs GIOS [10] and TRIM [11] taking the kinematics and effects of energy and small-angle straggling into account.

The solid lines in Fig. 3 are the result of distorted-wave Born approximation (DWBA) calculations with the code PTOLEMY [12] for the reaction mechanism with spectroscopic factors from shell-model calculations and optical model parameters from Refs. [13,14]. Calculations with different potentials [15] gave variations of ~20% in the cross sections. A shell-model calculation was performed within a space containing the $f_{7/2}$, $f_{5/2}$, $p_{3/2}$, and $p_{1/2}$ orbitals with a Hamiltonian described in Ref. [1]. The configurations included 0, 1, and 2 particles excited out of the $f_{7/2}$ orbital. These calculations yield spectroscopic factors of $S = 0.91(2p_{3/2})$, $S = 0.91(1f_{5/2})$, and $S = 0.90(2p_{1/2})$. With these spectroscopic factors, good agreement between the experimental and the calculated angular distributions is obtained, indicating that these states in ^{57}Ni are indeed well characterized as the $2p_{3/2}$, $2p_{1/2}$, and $1f_{5/2}$ single-particle states. Based on the statistics and the lack of optical potential parameters for ^{56,57}Ni, the accuracy for determining the absolute spectroscopic factor is estimated to be about 50%. However, the low yields observed in the excitation energy region between 2–4 MeV, where higher-lying $1/2^-$, $3/2^-$, and $5/2^-$ states are expected, support the fact that the main single-particle strength for these low-spin states is concentrated in the first three excited states.

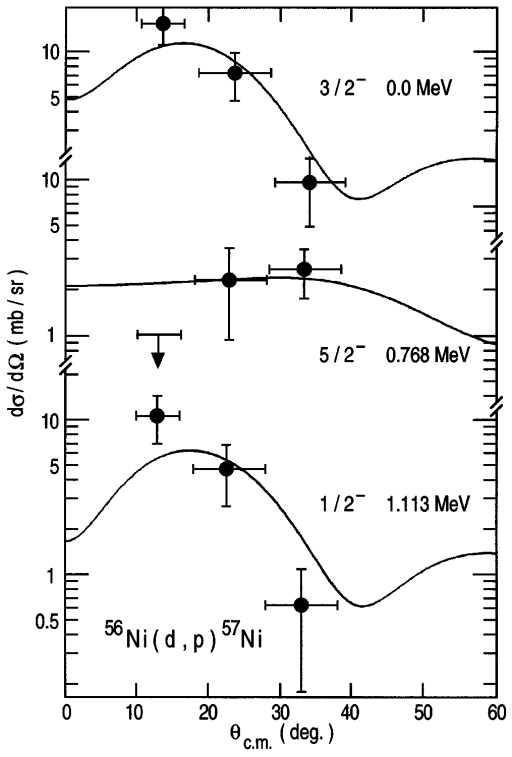

FIG. 3. Differential cross section $(\mathrm{d}\sigma/\mathrm{d}\Omega)_{\mathrm{cm}}$ as a function of the center-of-mass angle θ_{cm} for the three lowest states populated in the $d(^{56}\mathrm{Ni}, p)^{57}\mathrm{Ni}$ reaction. The solid lines are the result of DWBA calculations with spectroscopic factors from shell-model calculations.

The observation of the single-particle structure in ^{57}Ni allows us to make predictions for the strength of the $^{56}\mathrm{Ni}(p, \gamma)^{57}\mathrm{Cu}$ reaction leading to the mirror nucleus ^{57}Cu, which is crucial for the production of heavier proton-rich nuclei in explosive nucleosynthesis [16]. Because of the low Q value, the yield of the radiative capture reaction depends on the excitation energies and the spectroscopic strengths of specific low-lying states in ^{57}Cu. At the temperatures occurring in typical nova and supernova explosions and in x-ray bursts ($T_9 \sim 0.5$–1, where T_9 is the temperature measured in 10^9 K), the main contribution comes from the low-lying ($E_x \leq 3$ MeV) $5/2^-$ and $1/2^-$ states. Assuming charge symmetry and using the same spectroscopic factors C^2S as measured for the mirror nucleus ^{57}Ni, we estimate the proton widths Γ_p for proton-unbound mirror states in ^{57}Cu from the expression $\Gamma_p(E, l) = C^2S\Gamma_p^{\mathrm{s.p.}}(E, l)$. The single-particle widths $\Gamma_p^{\mathrm{s.p.}}(E, l)$ were calculated in a Woods-Saxon potential with a radius parameter of $r_0 = 1.25$ fm and a diffuseness of $a = 0.65$ fm or from R-matrix theory using a radius of 5.36 fm [17]. The excitation energies of these states were determined recently [18].

The astrophysical reaction rate $N_A\langle\sigma v\rangle$ for the $^{56}\mathrm{Ni}(p, \gamma)^{57}\mathrm{Cu}$ reaction is then given by

$$N_A\langle\sigma v\rangle = N_A\left(\frac{2\pi}{\mu kT}\right)^{3/2}\sum_{\mathrm{res}}\omega\gamma\exp\left(-\frac{E_r}{kT}\right), \quad (1)$$

where N_A is Avogadro's number, $\omega\gamma = \omega\frac{\Gamma_p\Gamma_\gamma}{\Gamma_p+\Gamma_\gamma}$ (the resonance strength), and ω is the statistical factor. The values for Γ_p (from this experiment), for Γ_γ (taken from Ref. [18]), and for the resonance strengths $\omega\gamma$ used in the rate calculations are summarized in Table I. There is good agreement between the two methods used for calculating the proton widths, especially for the important $1/2^-$ state at $E_x = 1.106$ MeV. Also included in Table I are the values of Γ_p from Ref. [18].

TABLE I. Excitation energies, resonance energies, spectroscopic factors, widths (calculated using R-matrix [RM] theory or a Woods-Saxon [WS] potential), and resonance strengths for the astrophysical reaction rate calculations. For comparison, the last column gives the proton widths calculated in Ref. [18].

J^π	E_x (MeV)	E_r (MeV)	C^2S	Γ_p^{RM} (eV)	Γ_p^{WS} (eV)	Γ_γ^* (eV)	$\omega\gamma^{\mathrm{RM}}$ (eV)	Γ_p^* (eV)
$5/2^-$	1.028	0.333	0.9	9.1×10^{-12}	5.6×10^{-12}	3.8×10^{-6}	2.7×10^{-11}	6.1×10^{-13}
$1/2^-$	1.106	0.411	0.9	1.9×10^{-7}	1.8×10^{-7}	1.3×10^{-2}	1.9×10^{-7}	1.5×10^{-8}
$5/2^-$	2.398	1.703	<0.2	<1	<0.8	2.3×10^{-2}	6.9×10^{-2}	8.5×10^{-2}
$7/2^-$	2.520	1.825	<0.2	<2.5	<1.6	1.3×10^{-2}	5.2×10^{-2}	7.0×10^{-2}

*From Ref. [17].

The astrophysical reaction rates are shown in Fig. 4 as a function of the temperature T_9. Since the proton widths are much smaller than the γ widths, the yield from the first two ($5/2^-$ and $1/2^-$) resonances is proportional to these widths and not sensitive to the precise values of the γ widths. In the temperature region $T_9 < 1$, the $1/2^-$ state completely dominates (see dot-dashed line in Fig. 4). Higher-lying states in ^{57}Cu with $E_x > 2.5$ MeV contribute only at temperatures $T_9 > 1$. The thin solid line in Fig. 4 represents the result for the astrophysical reaction rate obtained in Ref. [18]. Since these authors used a smaller proton width for the $1/2^-$ state, their estimate of the reaction rate for the $^{56}\mathrm{Ni}(p,\gamma)^{57}\mathrm{Cu}$ reaction is lower by more than an order of magnitude in the temperature region below $T_9 = 1$.

This work was supported by U.S. Department of Energy, Nuclear Physics Division, under Contract No. W-31-109-ENG-38, the National Science Foundation, and by a University of Chicago/Argonne National Laboratory Collaborative Grant.

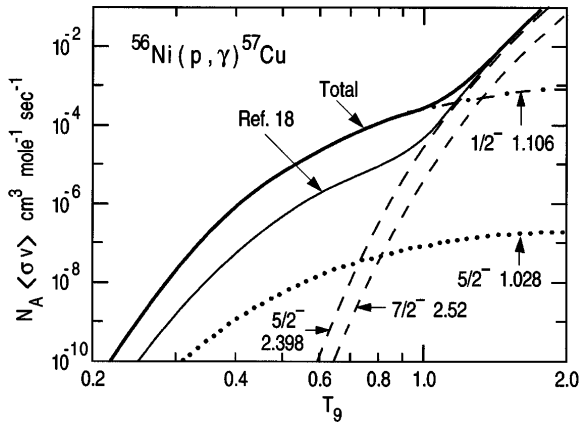

FIG. 4. Astrophysical reaction rates $N_A\langle\sigma v\rangle$ for the $^{56}\mathrm{Ni}(p,\gamma)^{57}\mathrm{Cu}$ reaction calculated with the resonance strengths $\omega\gamma$ given in Table I. The contributions from various low-lying states are presented. The total rate is also compared with that of Ref. [18].

[1] G. Kraus *et al.*, Phys. Rev. Lett. **73**, 1773 (1994).
[2] F. J. Eckle *et al.*, Nucl. Phys. **A506**, 159 (1990).
[3] C. R. Gould, D. P. Balamuth, P. F. Hinrichsen, and R. W. Zurmühle, Phys. Rev. **188**, 1792 (1969).
[4] R. K. Wallace and S. E. Woosley, Astrophys. J. Suppl. **45**, 389 (1981).
[5] *Landolt-Börnstein*, edited by H. Schopper, New Series I Vol. 13a (Springer-Verlag, Berlin, 1991) p. 330.
[6] National Electrostatics Corporation, Graber Road, Box 310, Middleton, WI 53562.
[7] C. N. Davids *et al.*, Nucl. Instrum. Methods Phys. Res., Sect. B **70**, 358 (1992).
[8] W. Henning *et al.*, Nucl. Instrum. Methods **184**, 247 (1981).
[9] K. E. Rehm *et al.*, Nucl. Instrum. Methods (to be published).
[10] H. Wollnik, J. Brezina, and M. Berz, Nucl. Instrum. Methods Phys. Res., Sect. A **258**, 408 (1987).
[11] J. F. Ziegler, J. B. Biersack, and U. Littmark, *The Stopping and Range of Ions in Solids* (Pergamon Press, New York, 1985).
[12] M. H. MacFarlane and S. C. Pieper, Argonne National Laboratory Report No. ANL-76-11(Rev. 1), 1978 (unpublished).
[13] J. A. R. Griffith, M. Irshad, O. Karban, and S. Roman, Nucl. Phys. **A146**, 193 (1970).
[14] A. Marinov, L. L. Lee, and J. P. Schiffer, Phys. Rev. **145**, 852 (1966).
[15] C. M. Perey and F. G. Perey, At. Data Nucl. Data Tables **17**, 1 (1976).
[16] A. E. Champagne and M. Wiescher, Annu. Rev. Nucl. Part. Sci. **42**, 39 (1992).
[17] J. P. Schiffer, Nucl. Phys. **46**, 246 (1964).
[18] X. G. Zhou *et al.*, Phys. Rev. C **53**, 982 (1996).